Conformational Change in the 16S rRNA in the *Escherichia coli* 70S Ribosome Induced by P/P- and P/E-Site tRNA^{Phe} Binding†

James W. Noah,‡ Tatjana G. Shapkina, Kavita Nanda, Wayne Huggins, and Paul Wollenzien*

Department of Molecular and Structural Biochemistry, North Carolina State University, Raleigh, North Carolina 27695-7622

Received August 1, 2003; Revised Manuscript Received October 10, 2003

ABSTRACT: The effects of P/P- and P/E-site tRNA^{Phe} binding on the 16S rRNA structure in the *Escherichia coli* 70S ribosome were investigated using UV cross-linking. The identity and frequency of 16S rRNA intramolecular cross-links were determined in the presence of deacyl-tRNA^{Phe} or *N*-acetyl-Phe-tRNA^{Phe} using poly(U) or an mRNA analogue containing a single Phe codon. For *N*-acetyl-Phe-tRNA^{Phe} with either poly(U) or the mRNA analogue, the frequency of an intramolecular cross-link C967 × C1400 in the 16S rRNA was decreased in proportion to the binding stoichiometry of the tRNA. A proportional effect was true also for deacyl-tRNA^{Phe} with poly(U), but the decrease in the C967 × C1400 frequency was less than the tRNA binding stoichiometry with the mRNA analogue. The inhibition of the C967 × C1400 cross-link was similar in buffers with, or without, polyamines. The exclusive participation of C967 with C1400 in the cross-link was confirmed by RNA sequencing. One intermolecular cross-link, 16S rRNA (C1400) to tRNA^{Phe}(U33), was made with either poly(U) or the mRNA analogue. These results indicate a limited structural change in the small subunit around C967 and C1400 during tRNA P-site binding sensitive to the type of mRNA that is used. The absence of the C967 × C1400 cross-link in 70S ribosome complexes with tRNA is consistent with the 30S and 70S crystal structures, which contain tRNA or tRNA analogues; the occurrence of the cross-link indicates an alternative arrangement in this region in empty ribosomes.

The interactions of the tRNAs with the ribosome have been investigated with a succession of methods over the last 20 years. Nucleotides in the rRNAs that become chemically nonreactive upon tRNA binding were identified, and many of these have been shown to be involved in contacts with tRNA (*1*−*3*). Many more of the details of the ribosome−tRNA interactions have been determined by crystallography and cryo-EM.[1] These include the description of the arrangements of 16S rRNA elements that stabilize the P-site-bound tRNA on the 30S subunit (*4*−*7*), the interaction between the 16S rRNA and the A-site-bound tRNA that is dependent on the codon−anticodon interaction in the A-site (*5*, *6*, *8*, *9*), the conformation of the tRNA in the ternary complex during A-site accommodation (*10*, *11*), and 23S rRNA−tRNA interactions that provide the orientation of the aminoacyl- and peptidyl-containing ends of the tRNAs in the peptidyl transferase center (*6*, *12*). The ribosome has conformational flexibility, particularly in the 30S subunit, that accompanies many of the steps in tRNA and factor binding. This includes rotation and bending of the head and changes in the platform region of the 30S subunit upon subunit association (*13*, *14*), a tightening of the 30S subunit structure during tRNA accommodation (*9*), concerted structural changes during the translocation reaction (*14*−*16*), and changes induced by initiation factor 3 binding (*17*).

An issue that complicates structural experiments is the known ribosome dependence on the ionic environment. Conventional buffers contained monovalent (K^+ or NH_4^+) and divalent cations (Mg^{2+}) to maximize ribosome activity and minimize nonspecific tRNA binding (*18*−*22*). tRNA footprinting experiments done under these conditions led to the proposal of the hybrid states model for translocation (*2*, *23*, *24*), and these conditions have been used in kinetic experiments (*25*, *26*). The inclusion of polyamines such as spermine and spermidine increase in vitro protein synthesis speed and processivity (*27*, *28*); subsequently, polyamine buffers have also been used in tRNA protection experiments (*29*−*31*). Cryo-EM experiments with 70S·tRNA·mRNA complexes in conventional and polyamine buffers provided evidence for the redistribution in the equilibrium between P/P and P/E-site binding of deacyl-tRNA$_f^{Met}$ (*32*). Thus, ionic conditions can alter the details of some of the tRNA−ribosome interactions.

UV cross-linking is used here to compare the 16S rRNA conformation in the empty 70S ribosome and its conformation with P-site bound tRNA. Previously, we demonstrated that UV-induced cross-linking can detect conformational differences in the 16S rRNA, particularly near nucleotide residues involved in interactions in the decoding region of

† Supported by National Institutes of Health Grant GM43237 to P.W. and by a GAANN Fellowship to J.W.N.

* Corresponding author. Telephone (919) 515-5703. Fax (919) 515-2047. E-mail: paul_wollenzien@ncsu.edu.

‡ Present address: Institute for Cellular and Molecular Biology, Department of Chemistry and Biochemistry, and Section of Molecular Genetics and Microbiology, School of Biological Sciences, University of Texas at Austin, Austin, TX 78712.

[1] Abbreviations: β-ME, β-mercaptoethanol; bis-Tris, bis (2-hydroxyethyl) imino-tris(hydroxymethyl) methane; cryo-EM, cryo-electron microscopy; EDTA, ethylenediaminetetraacetic acid; HEPES, 4-(2-hydroxyethyl)-1-piperazineethanesulfonic acid; NAcPhe-tRNA^{Phe}, *N*-acetylphenylalanyl-tRNA^{Phe}; Phe-tRNA^{Phe}, phenylalanyl-tRNA^{Phe}; poly(U), poly-uridine mRNA; rRNA, ribosomal RNA; Tris, tris(hydroxymethyl)-aminomethane.

10.1021/bi035369q CCC: $25.00
Published on Web 11/14/2003

the subunit. Cross-linked nucleotides associated with the tRNA P-site were significantly and specifically affected by changes in the Mg^{2+} concentration and subunit association, while cross-links in other parts of the 16S rRNA were unaffected (*33*, *34*). The two internal cross-links that were most responsive are C967 × C1400 and C1402 × C1501. In the present paper, the structural response in 70S ribosomes complexed with deacylated or acylated $tRNA^{Phe}$ and with different messenger RNA and buffers has been investigated. The data demonstrate a specific inhibition of the 16S rRNA cross-link C967 × C1400 close to the decoding region in response to P/P, and in some cases, P/E-site binding, indicating that an adjustment is made by the 30S subunit during tRNA binding.

MATERIALS AND METHODS

Preparation of Ribosomes and UV Cross-Linking Procedures. Escherichia coli 70S ribosomes and ribosomal subunits were prepared and stored according to Makhno et al. (*35*). Reassociation of 30S and 50S ribosomal subunits was done in solutions containing either conventional buffer (20 mM Tris-HCl, pH 7.5, 100 mM NH_4Cl, 10 mM $MgCl_2$, 6 mM β-ME) or polyamine buffer (20 mM HEPES-KOH, pH 7.8, 150 mM NH_4Cl, 6 mM $MgCl_2$, 2 mM spermidine, 0.4 mM spermine, 6 mM β-ME) (*29*). Complexes were formed by incubating 70S ribosomes with mRNA and tRNA for 30 min at 37 °C. They were then placed on ice for 10 min and irradiated at 4 °C. Irradiation was completed with a 312 nm trans-illuminator (Fotodyne, Inc., Hartland, WI) for 20 min as previously described (*36*). After irradiation, rRNA was recovered from the samples by proteinase K digestion, followed by phenol extraction, ether extraction, and ethanol precipitation. The RNA was dephosphorylated with shrimp alkaline phosphatase (USB, Cleveland, OH), phenol extracted, ether extracted, and ethanol precipitated. 16S rRNA was isolated on 1% agarose gels and then was 5′ end-labeled with [γ-^{32}P] ATP by T4 polynucleotide kinase (MBI Fermentas, Hanover, MD) or 3′ end-labeled with [5′-^{32}P] pCp by T4 RNA ligase (*41*).

Cross-linked 16S rRNA was separated by gel electrophoresis on gels made with 3.6% acrylamide/bis-acrylamide (70:1), 8.3 M urea, and BTBE buffer (30 mM bis-Tris, 30 mM boric acid, 2.5 mM EDTA, pH 6.8) as previously described (*36*). For purification, the locations of bands containing uncrosslinked and cross-linked 16S rRNA were detected with a PhosphorImager (Amersham, Piscataway, NJ). Bands were cut out and eluted by ultracentrifugation through 2 M CsCl, 0.2 M EDTA, pH 7.4, for 16 h at 40 000 rpm (*37*). RNA pellets were redissolved in 250 μL of H_2O, phenol extracted, ether extracted, and ethanol precipitated before further analysis.

Preparation of N-Acetyl-PhetRNA^{Phe}. Ten A_{260} units of *E. coli* deacyl-$tRNA^{Phe}$ (Sigma, St. Louis, MO) was aminoacylated according to Rheinberger et al. (*38*) using bovine mitochondrial tRNA synthetase (*39*). After two ethanol precipitations to remove excess phenylalanine, the sample was purified by HPLC on a PRP-1 reverse-phase column (Hamilton) with a 0−20% acetonitrile gradient in 0.1 M NaOAc, 10 mM $MgCl_2$, pH 5.1. After phenol extraction and ethanol precipitation, the Phe-$tRNA^{Phe}$ was incubated with 30 mg of acetic acid *N*-hydroxysuccinimide ester (Sigma, St. Louis, MO) in 80% DMSO (0.5 mL total volume) for 2 h on ice (*40*). Following acylation, the sample was ethanol precipitated twice, dried, dissolved in H_2O, and stored at −20 °C.

tRNA^{Phe} Binding to Ribosomes. Complexes for analytical experiments contained 40 pmol of ribosomes, 10 μg of poly(U) or 200 pmol of mRNA, and either 40 or 200 pmol of $tRNA^{Phe}$ in 100 μL total volume in conventional buffer or polyamine buffer. The mRNA analogue used in the experiments is 54 nucleotides containing the sequence GGCGAUAACACUC-AGGAGAUAAUAA**AUGUUU**ACAGCUGAUCAAUCG-UGCAUCCA in which a Shine Dalgarno sequence is underlined, and the codons AUG and UUU are bold. It was made by in vitro transcription using the conditions for high yield of RNA (*41*). Preparative samples contained 200 pmol of ribosomes, 50 μg of poly(U) or 1000 pmol of mRNA, and 400 pmol of $tRNA^{Phe}$ or NAcPhe- $tRNA^{Phe}$ in 200 μL. Samples were incubated for 30 min at 37 °C, stored on ice for 10 min, and irradiated as stated previously. The stoichiometry of tRNA binding was determined by chemically modifying 70S-tRNA complexes with kethoxal (*42*). G926 is normally hyperreactive to kethoxal modification but becomes protected by P/P- or P/E-site binding (*2*, *5*). The extent of protection as compared to unmodified 16S rRNA and modified empty 70S was used as an index of P-site binding.

Determination of Cross-Link Identity and Frequency. Cross-linked RNA was separated by gel electrophoresis on denaturing 3.6% polyacrylamide gels as described previously. Cross-linking sites were found by primer extension analysis using 11 DNA primers complementary to regions throughout 16S rRNA (*36*). The frequency of cross-linking was determined from phosphorImager data (Amersham, Piscataway, NJ) of duplicate independent experiments. To normalize for RNA loading, the cross-link band intensity was referenced to the same cross-link band (C54 × C352) in each respective lane. The C54 × C352 band showed less than 10% variance in all lanes when normalized to the uncross-linked 16S rRNA parent band in the same lane, determined after short exposure.

Determination of the C967 Cross-Linking Site by RNA Sequencing. RNA was prepared from cross-linked empty 70S ribosomes as described previously. The oligonucleotide 5′$_m$C$_m$G$_m$C$_m$UdTdGdTdG$_m$C$_m$G$_m$G$_m$G$_m$C$_m$C$_m$C$_m$C3′ was used with RNase H to direct a specific cut between nucleotide 936 and 937. Specifically, 320 μg of total rRNA from irradiated 70S ribosomes and 50 pmol of oligonucleotide were mixed in 20 mM Tris HCl, pH 7.8, 63.5 mM NH_4Cl in 200 μL total volume, heated for 5 min at 55 °C, and cooled to 20 °C over a period of 15 min. Then, 30 μL of 10 mM $MgCl_2$ and 20 units of RNase H (USB, Cleveland, OH) were added in that order, and after incubation for 10 min at 55 °C, the sample was phenol and ether extracted and ethanol precipitated. The RNA was treated with 45 units of shrimp alkaline phosphatase in 200 μL total volume in 20 mM Tris HCl, pH 8.0, 10 mM $MgCl_2$ for 15 min at 37 °C and then was phenol extracted, ether extracted, and ethanol precipitated. The 605-nucleotide fragment was isolated by separation on 1% agarose gel. Purified fragments (usually 15−20 μg) were 5′ labeled with 60 units of T4 polynucleotide kinase using 0.66 mCi γ [^{32}P] ATP in 200 μL total volume containing 50 mM Tris HCl, pH 7.5, 1 mM $MgCl_2$, 10 mM β-ME for 30 min at 37 °C. Samples were phenol extracted, ether extracted, and ethanol precipitated twice to remove

unincorporated [^{32}P] ATP. Cross-linked RNA was separated by electrophoresis on 5% polyacrylamide gels (40:1 acrylamide/bisacrylamide), 8.3 M urea, and BTBE buffer. Bands containing linear RNA and cross-linked RNA were identified using a phosphorimager and were cut out and collected by ultracentrifugation (40 000 rpm for 28 h) through a 4 mL cushion of 2 M CsCl, 0.2 M EDTA, pH 7.0 in a Ti 50.2 angle rotor (Beckman Coulter, Fullerton, CA). Twenty micrograms of herring sperm DNA (Sigma, St. Louis, MO) was added to the CsCl solution to make a visible pellet. Pellets were redissolved in 200 μL of 10 mM Tris HCl, pH 8.0, 1 mM EDTA, 1% SDS and were phenol and ether extracted, ethanol precipitated, and redissolved in H_2O to give 2000 cpm/μL. Partial alkaline hydrolysis and RNase T1 digestion were done as described for tRNA.

Determination of Cross-Linking Site in tRNA^{Phe}. Deacylated tRNA^{Phe} was 3′ labeled with 5′[^{32}P]pCp and T4 RNA ligase for use in ribosome complexes. Irradiation and purification of 16S-sized RNA was done as described previously. RNA was separated on a denaturing 3.6% polyacrylamide gel as described previously. RNA was isolated from gel regions containing [^{32}P]-labeled tRNA^{Phe}, and this was subjected to partial hydrolysis and sequencing to determine the site(s) of cross-linking. RNA samples were incubated in hydrolysis buffer (25 mM Na_2CO_3, pH 9.0, 0.5 mM EDTA) for 3 min at 90 °C for partial hydrolysis (*41*), and RNase T1 sequencing was performed on control and cross-linked tRNA as described (*41*). All samples were immediately cooled to 0 °C and analyzed by gel electrophoresis on denaturing 12% polyacrylamide gels.

RESULTS

Effects of tRNA^{Phe} Binding on 16S rRNA Intramolecular Cross-Link Identity and Frequency. Deacyl-tRNA^{Phe} and *N*-acetyl-Phe-tRNA^{Phe} were bound to 70S ribosomes to determine if they would affect the frequency or identity of any UV-induced 16S rRNA cross-links. Complexes were prepared with poly(U) or with an mRNA analogue under conditions in which tRNA binding is message dependent (*24*). Both conventional and polyamine buffer systems were used in these experiments.

In the first experiment, empty 70S ribosomes or complexes made with either poly(U) or mRNA and deacyl-tRNA^{Phe} at a 2:1 molar ratio of tRNA/ribosomes were irradiated. 16S-sized RNA was isolated on agarose gels and was then [^{32}P]-labeled and examined by gel electrophoresis on a denaturing polyacrylamide gel (Figure 1A). One difference in samples containing tRNA, as compared to samples from empty ribosomes, is the absence of a band labeled I in Figure 1A in the top part of the gel. RNA was isolated from region I in all six samples and was analyzed by reverse transcription. Reverse transcription stops occur at 16S rRNA nucleotides that indicate a cross-link involving C967 and C1400 in the empty 70S ribosome samples; these stops disappear nearly completely in the RNA from 70S·tRNA·mRNA and the 70S·tRNA·poly(U) complexes (Figure 1B,C). Poly(U) or the mRNA analogue incubated with 70S ribosomes without tRNA do not alter the frequency of the C967 × C1400 cross-link (results not shown). In this particular gel, the band at I appears to be a doublet, but no additional reverse transcription stops were identified in the RNA from region I. A second difference in the sample from the complex made with the mRNA analogue is the appearance of a band labeled II in the bottom third of the polyacrylamide gel. A reverse transcription stop occurs at C1397 in the samples that contain the mRNA analogue (Figure 1D), so this RNA species may be similar to the product from a similar location in the gel electrophoresis pattern that was shown to contain a cross-link between 16S (C1397) and mRNA at position +7 (with respect to the A of AUG being +1) (*44*).

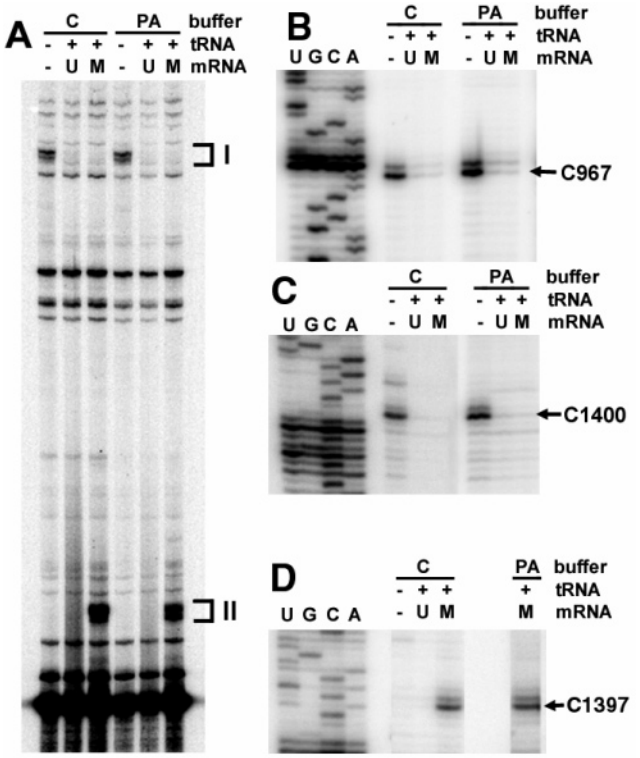

FIGURE 1: Inhibition of the C967 × C1400 cross-link by tRNA binding. (A) 70S ribosomes or 70S ribosomes incubated with excess poly(U) (designated U) or mRNA analogue (designated M) and 2:1 molar ratio of deacyl-tRNA^{Phe} to 70S ribosomes were irradiated with UV light, and 16S-sized RNA was isolated, 5′ [^{32}P]-labeled, and electrophoresed on a denaturing 3.6% polyacrylamide gel. RNA from the regions marked I and II was isolated from the samples for further analysis. (B) Reverse transcription of RNA I in the interval 957−976. The RNA sequence is indicated by lanes marked U, C, G, and A. In this and subsequent reverse transcription experiments, the reverse transcription stop sites are labeled for the adjacent nucleotide at which the cross-link occurs. The arrow points to the strong reverse transcription stop at A968 corresponding to a cross-link at C967. (C) Reverse transcription of RNA I in the interval 1389−1411. The arrow points to the strong reverse transcription stop at G1401 corresponding to a cross-link at C1400. (D) Reverse transcription of RNA II in the interval 1388−1402. The arrow points to the strong reverse transcription stop at A1398 corresponding to a cross-link at C1397.

Complexes were made with poly(U) and a 1:1 and a 5:1 molar ratio of tRNA/ribosomes to determine if there is a quantitative connection between tRNA binding and frequency changes in cross-linking. As shown in Figure 2A, a band in the upper part of the pattern again is decreased in samples containing tRNA. This band will be shown to contain C967 × C1400 in the next section. Bands containing other intramolecular 16S rRNA cross-links were quantified and did not change. With both molar ratios of deacyl-tRNA^{Phe}/70S ribosomes, there was almost a complete disappearance of the C967 × C1400 cross-link in both sets of samples (Figure 2A, lanes 3, 4, 9, and 10; Table 1). The C967 ×

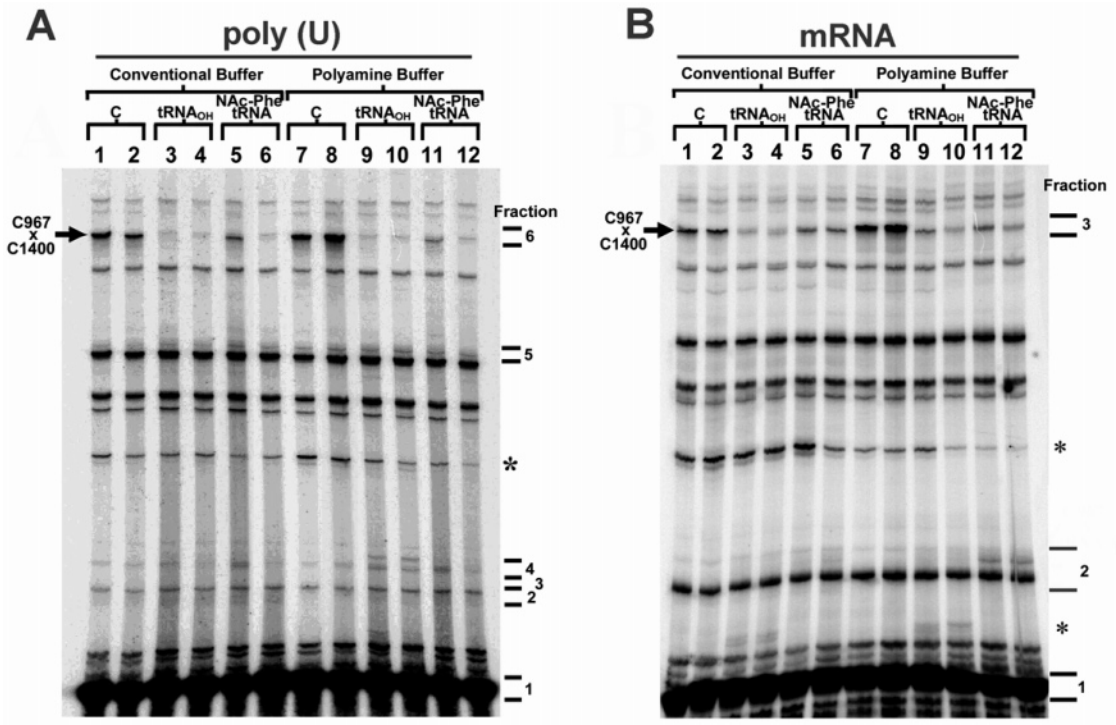

FIGURE 2: Titration of 70S ribosomes with tRNA^{Phe} and effects on 16S rRNA cross-linking frequency. (A) Lanes 1−6 and 7−12 contain samples cross-linked in conventional and polyamine buffer, respectively, using poly(U) to program tRNA^{Phe} binding. Lanes 1 and 7 contain RNA from empty ribosomes. Lanes 2 and 8 contain samples prepared with poly(U) but no tRNA^{Phe}. Lanes 3−4, 9, and 10 contain samples prepared with 1:1 and 5:1 molar ratios of deacyl-tRNA^{Phe}/70S ribosomes. Lanes 5−6, 11, and 12 contain samples prepared with 1:1 and 5:1 molar ratios of *N*-acetyl-Phe-tRNA^{Phe}/70S ribosomes. (B) Lanes 1−6 and 7−12 show samples cross-linked in conventional and polyamine buffer, respectively, using the mRNA analogue to program tRNA^{Phe} binding. Lanes 1 and 7 contain experiments on empty ribosomes. Lanes 2 and 8 contain mRNA but no tRNA^{Phe}. Lanes 3, 4, 9, and 10 contain samples prepared with 1:1 and 5:1 molar ratios of deacyl-tRNA^{Phe}/70S ribosomes. Lanes 5, 6, 11, and 12 contain samples prepared with 1:1 and 5:1 molar ratios of *N*-acetyl-Phe-tRNA^{Phe}/70S ribosomes. The 16S rRNA cross-link C967 × C1400 is indicated by a labeled arrow to the left. Regions of preparative gels excised to obtain RNA for the reverse transcription experiments shown in Figure 3 are indicated to the right. The bands indicated by the asterisk (*) were not seen in duplicate experiments.

Table 1: 16S rRNA G926 Protection and 16S rRNA Crosslink C967 × C1400 Frequency Decrease Induced by tRNA

		conventional buffer			polyamine buffer		
tRNA/mRNA	ratio tRNA:ribosomes	0:1 (%)	1:1 (%)	5:1 (%)	0:1 (%)	1:1 (%)	5:1 (%)
tRNA$^{Phe}_{OH}$ + poly(U)	G926 protection[a]	0	93	94	0	94	94
	C967 × C1400 frequency decrease[b]	0	90	99	0	91	99
tRNA$^{Phe}_{OH}$ + mRNA	G926 protection[a]	0	93	98	0	95	95
	C967 × C1400 frequency decrease[b]	0	59	63	0	53	65
N-acetyl-Phe-tRNA^{Phe} + poly(U)	G926 protection[a]	0	48	80	0	46	79
	C967 × C1400 frequency decrease[b]	0	56	87	0	82	98
N-acetyl-Phe-tRNA^{Phe} + mRNA	G926 protection[a]	0	43	41	0	43	50
	C967 × C1400 frequency decrease[b]	0	32	39	0	55	65

[a] Values for G926 protection by P-site tRNA indicate percent of binding of tRNA into the P/P- or P/E-site. These were taken from chemical probing experiments that evaluated the extent of reaction of kethoxal at G926. [b] Values for C967 × C1400 cross-link frequencies were taken from gel electrophoresis analysis of 16S rRNA cross-linking. Uncertainties are about 10% of the indicated values.

C1400 frequency decrease is somewhat less when *N*-acetyl-Phe-tRNA^{Phe} is bound using poly(U) as the messenger (Figure 2A, lanes 5, 6, 11, and 12).

The quantitative effects of deacyl-tRNA^{Phe} and *N*-acetyl-Phe-tRNA^{Phe} binding to the 70S ribosome directed by the mRNA analogue were also determined. As shown in Figure 2B, titration experiments were carried out with deacyl-tRNA^{Phe} in conventional (lanes 3 and 4) and polyamine buffers (lanes 9 and 10) and with *N*-acetyl-Phe-tRNA^{Phe} in conventional (lanes 5 and 6) and polyamine buffers (lanes 11 and 12).

tRNA binding stoichiometries for deacyl-tRNA^{Phe} and *N*-acetyl-Phe-tRNA^{Phe} in the presence of poly(U) or the mRNA analogue were determined by measuring the degree of protection of G926 to kethoxal reaction (results not shown). G926 normally is hyper-reactive with kethoxal in the empty ribosome. However, tRNA bound to the P-site in the 30S subunit in either the P/P or the P/E states (*1*, *2*) blocks this reaction and can be used to quantify the binding of tRNA regardless of the hybrid state. The fractional occupation for each of the conditions is summarized in Table 1. In all complexes containing poly(U) and *N*-acetyl-Phe-tRNA^{Phe} or deacyl-tRNA^{Phe}, there was a direct correlation between the extent of tRNA binding and the decrease in the C967 × C1400 cross-link. This is also true for complexes containing the mRNA analogue and *N*-acetyl-Phe-tRNA^{Phe}.

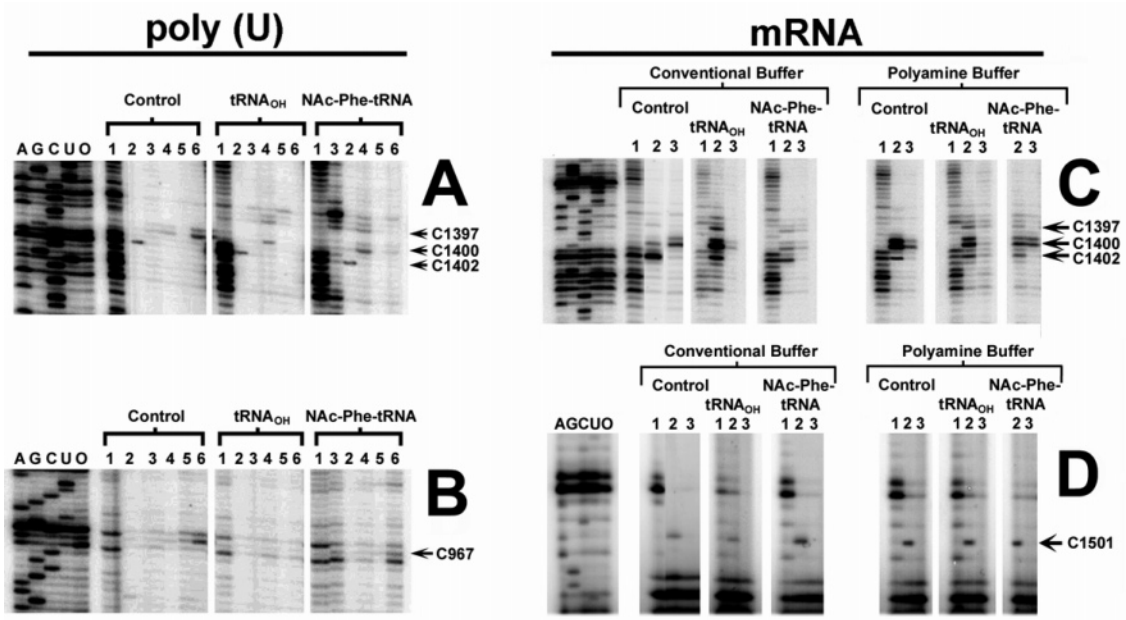

FIGURE 3: Reverse transcription analysis of UV induced cross-links in 16S rRNA in 70S·tRNA^{Phe} complexes. Panels A and B contain analyses of experiments performed on empty ribosomes (control), and with deacyl-tRNA^{Phe} (tRNA$_{OH}$) and *N*-acetyl-Phe-tRNA^{Phe} (NAc-Phe-tRNA) using poly(U) in conventional buffer. Samples in lanes 1−6 are from fractions excised from preparative gels according to Figure 2A. (A) Primer extension in the 16S rRNA interval 1389−1410. Reverse transcription stops at C1397, C1400, and C1402 are indicated to the right of panel A by arrows. The lanes to the left of the gel, indicated by A, G, C, U, and O, in panels A−D are sequence lanes and unirradiated control lanes, respectively. (B) Reverse transcription analysis in the interval 959−976. Panels C and D contain samples from experiments on empty ribosomes (control), with deacyl-tRNA^{Phe} (tRNA$_{OH}$), *N*-acetyl-Phe-tRNA^{Phe} (NAc-Phe-tRNA), and mRNA in conventional and polyamine buffer as indicated. Lanes 1−3 in each set use RNA fractions excised from the preparative gel in Figure 2B. (C) Reverse transcription analysis in the 16S rRNA interval 1386−1410. Reverse transcription stops are indicated on the side of the gel at positions C1397, C1400, and C1402. (D) Reverse transcription analysis in the interval 1495−1506. The reverse transcription stop for the cross-link C1501 is indicated.

However, in the four experiments that use the mRNA analogue and deacyl-tRNA^{Phe}, there was a smaller decrease in the cross-link frequency than would be expected from the binding stoichiometry. A-site binding may occur in the experiments with poly(U) and the 5:1 tRNA to ribosome input ratio. However, this should not be the case for the 1:1 input ratio or for the experiments with mRNA analogue, so a significant effect by tRNA in the A-site can be ruled out. For *N*-acetyl-Phe-tRNA^{Phe} and poly(U) in polyamine buffer at 1:1, there was a somewhat larger decrease in the C967 × C1400 than would be expected from the amount of P-site tRNA binding. This response was not seen for the same tRNA in conventional buffer and was not seen with mRNA, so the difference seen in the one case may not be quantitatively significant.

Deacyl-tRNA^{Phe} binding and C967 × C1400 cross-link frequency were measured in conventional buffer with a high Mg^{2+} concentration with, and without, mRNA to determine the cross-link dependence on mRNA. tRNA binding stoichiometries and the decreases in the C967 × C1400 cross-link frequency are summarized in Table 2. In the $T_{20}A_{100}M_{20}$ buffer that was used, decreases in the cross-link frequency are proportional to tRNA binding as contrasted to a less than proportional response that is seen in the $T_{20}A_{100}M_{10}$ buffer. Furthermore, the decrease in the frequency of the C967 × C1400 cross-link is the same without or with the mRNA.

Reverse Transcription Analysis of Cross-Links in the 16S rRNA Decoding Region. Reverse transcription analyses were performed on RNA from complexes that were made in reactions containing a 2:1 molar ratio of deacyl-tRNA^{Phe} or *N*-acetyl-Phe-tRNA^{Phe} and poly(U) in conventional buffer to determine cross-linking sites. RNA from the irradiated complexes was first separated by gel electrophoresis, and RNA from regions 1−6 designated in Figure 2A was isolated for analysis. All samples were prepared from the same starting amounts of 70S ribosomes, and the RNA from all fractions (except fraction 1) was isolated and redissolved in the same volume prior to reverse transcription, so the intensity of the reverse transcription stops are a semiquantitative measure of cross-link frequency. The RNA in fraction 1 was redissolved in a 10-fold larger volume due to the large amount of linear 16S rRNA in the samples. Reverse transcription analysis in the 16S rRNA interval 1389−1410 in the decoding region is shown in Figure 3A. The control empty ribosome samples produce reverse transcription stops

Table 2: Dependence of G926 Protection and C967 × C1400 Decrease on mRNA under Conditions of High Mg^{2+} Concentration[a]

tRNA:70S input stoichiometry	1:1	5:1
−mRNA		
G926 protection[b] (%)	34	62
C967 × C1400 decrease[c] (%)	33	53
+mRNA		
G926 protection[b] (%)	54	90
C967 × C1400 decrease[c] (%)	58	88

[a] All measurements were done in buffers that contained 100 mM NH_4Cl and 20 mM $MgCl_2$ as well as 20 mM Tris HCl, pH 7.5 (or 80 mM NH_4 cacodylate, pH 7.2, for the kethoxal reactions). [b] Values for G926 protection by P-site tRNA indicate percent of binding of tRNA into the P/P- or P/E-site. These were taken from chemical probing experiments that evaluated the extent of reaction of kethoxal at G926. [c] Values for C967 × C1400 cross-link frequencies were taken from gel electrophoresis analysis of 16S rRNA cross-linking. Uncertainties are about 10% of the indicated values.

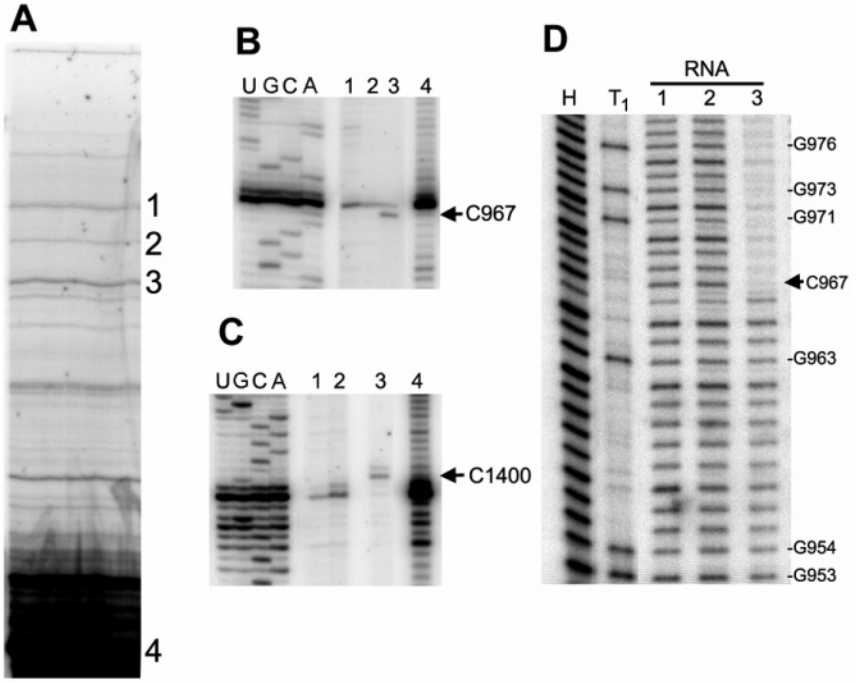

FIGURE 4: Confirmation of C967 as cross-linking site by RNA analysis. (A) Denaturing polyacrylamide gel electrophoresis of cross-linked molecules in 16S rRNA fragment 937−1542. RNA from empty irradiated 70S ribosomes was subjected to RNase H breakage between 16S rRNA nucleotides 936 and 937, and the 937−1542 fragment was isolated and 5′-labeled with [^{32}P] before electrophoresis on a denaturing 5% polyacrylamide gel. RNA from bands marked 1−4 was isolated for subsequent analysis. RNA from bands 1−3 contains internal cross-links, and RNA from band 4 contains linear RNA. (B and C) Identification of the band containing the C967 × C1400 cross-link. Reverse transcription of fractions 1−4 through intervals 955−974 and 1391−1411 are shown in panels B and C. RNA from band 3 produces reverse transcription stops for C967 and C1400 as indicated by the arrows. (D) Partial alkaline hydrolysis of cross-linked RNA fragments. Bands 1−3 were subjected to partial alkaline hydrolysis H to determine the location of any cross-links that interfere with the pattern of linear fragments originating from the 5′ end of the 937 nucleotide-sized RNA. Partial alkaline hydrolysis (H) and partial RNase T1 digestion (T1) of the band 4 linear RNA were used to determine the identity of the steps indicated by the identity of G residues in the ladder. The arrow points to position C967 that is the first nucleotide absent in the partial alkaline hydrolysis ladder in band 3 RNA.

at C1402 (control lane 2) and at C1400 (control lane 6) indicating the presence of cross-links C1402 × C1501 and C967 × C1400 (*36*). In the samples containing deacyl-tRNA or *N*-acetyl-phe-tRNA, reverse transcription stops were still seen at C1402 ($tRNA_{OH}$ lanes 2 and NAc-Phe-tRNA lanes 2); however, the stops at C1400 that would be part of the C967 × C1400 cross-link were not seen ($tRNA_{OH}$, lane 6) or are seen at reduced intensity (NAc-Phe-tRNA, lane 6). RNA from fraction 4 produced a stop at C1400 (to $tRNA^{Phe}$, described next). In addition, stops at C1397, A1396, and C1395 are present and may be due to cross-linking with poly(U). In the samples that contained NAc-Phe-tRNA, reverse transcription stops in the same pattern as those seen in the deacyl-$tRNA^{Phe}$ lanes were obtained (lanes 2 and 4). The region containing the C967 stop of the C967 × C1400 cross-link was also analyzed (Figure 3B), and the behavior of RNA in fraction 6 mirrored that of the C1400 stop in the fraction 6 RNA, confirming the inhibition of the C967 × C1400 cross-link in samples containing tRNA.

Reverse transcription analyses were also performed on fractionated samples from complexes containing the mRNA analogue and 2:1 molar ratios of deacyl-$tRNA^{Phe}$ or *N*-acetyl-Phe-$tRNA^{Phe}$ over 70S ribosomes. The reverse transcription analyses of 16S rRNA in the interval 1386−1410 and in the interval 1494−1506 are shown in Figure 3C,D. RNA from fractions 1−3 were obtained from the gel regions indicated to the right of the gel in Figure 2B. The relative intensity of the stops at position 1400 in fraction 3 in this set of samples is related to a cross-link frequency for the C967 × C1400 cross-link and decrease in the samples containing tRNA. Reverse transcription stops in fraction 2 at C1402 (part of the C1402 × C1501 cross-link) were present in the samples containing deacyl-$tRNA^{Phe}$ and *N*-acetyl-Phe-$tRNA^{Phe}$. Reverse transcription stops at 1397 in fraction 2 were seen and are consistent with 16S rRNA cross-linking to mRNA. Reverse transcription analysis in the interval 1494−1506 (Figure 3D) showed a stop at C1501 in fraction 2 that confirms the presence of the cross-link C1402 × C1501 in all of the samples.

Determination of the C967 Cross-Linking Site by RNA Analysis. Because the involvement of C967 with C1400 was considered unlikely given the arrangement of this region in the crystal structure (see Discussion), an additional determination of the C967 cross-linking site was done by RNA sequencing. RNA from irradiated empty 70S ribosomes was digested with RNase H with a mixed DNA−RNA oligonucleotide to induce strand breakage between nucleotides 936 and 937. After purification of the 605-nucleotide RNA by agarose gel electrophoresis, the 5′ end at 937 was labeled with [^{32}P]. The RNA was then separated on a denaturing polyacrylamide gel (Figure 4A), and RNAs were isolated from three prominent bands that might contain the C967 × C1400 cross-link. The RNA from band 3 was determined by reverse transcription to contain the C967 × C1400 cross-link (Figure 4B,C). The exact location of the cross-link around C967 was determined by partial alkaline hydrolysis and partial RNase T1 digestion (Figure 4D). The cross-linking site was identified by the disappearance of the regular

pattern of linear RNA fragments because of the branched structure at the cross-linked nucleotide. The patterns show corresponding bands in the cross-link and control sample up to and including G966, but after that position, the partial alkaline hydrolysis pattern abruptly disappeared in the RNA containing the cross-link. Densitometry of the band intensity as compared to the control sample indicated that all cross-linking in fraction 3 RNA involves C967.

Analysis of the 16S rRNA−tRNA Cross-Link. The increase in frequency of the C1400 reverse transcription in fractions close to the bottom of the polyacrylamide gel when tRNA was present in complexes suggested that 16S rRNA position C1400 was involved in a $tRNA^{Phe}$ cross-link. To further investigate this possibility, deacyl-$tRNA^{Phe}$ was 3′-labeled with 5′ [^{32}P]pCp and was bound to 70S ribosomes in the presence of either the mRNA analogue or poly(U). The samples were irradiated as in previous experiments, and 16S-sized RNA was purified on agarose gels. The RNA was analyzed by polyacrylamide gel electrophoresis without additional [^{32}P] labeling. The pattern of cross-linking in complexes with the mRNA analogue or poly(U) is shown in Figure 5A. For the 70S complex containing the mRNA analogue, one band of modest intensity, labeled 1 on the right of the gel, was seen in the bottom part of the gel but above the position of uncrosslinked linear 16S rRNA. For the 70S complexes containing poly(U), a series of bands was seen in the gel, the most frequent of which, labeled 2, was at the same position as band 1 the mRNA experiment. Additional bands above this are labeled 2a, 2b, and 2c. However, in subsequent experiments done with 70S ribosomes that had not been dissociated and reassociated, 2a, 2b, and 2c were absent, and the presence of 2a, 2b, and 2c is correlated to a low degree of breakage of the 23 S rRNA during handling of the ribosomes. Therefore, only RNA from bands 1 and 2 was further characterized as products involving cross-links between 16S rRNA and tRNA. The RNA from band 3 should contain some tRNA, but the majority of its mass should be uncrosslinked linear 16S rRNA.

Reverse transcription was done on the RNA from bands 1, 2, and 3 to confirm the 16S rRNA C1400 site as the nucleotide involved in the tRNA cross-link. The pattern of reverse transcription in the interval between 1391 and 1409 for the samples 1, 2, and 3 is shown in Figure 5B. Reverse transcription of samples 1 and 2 produced stops corresponding to a cross-link at C1400 not seen in the control sample 3. No other stops were seen in the samples attributable to tRNA cross-linking. This result is consistent with oligonucleotide-directed RNase H digestion of the cross-linked 5′ [^{32}P]-labeled tRNA and 16S rRNA, which determined that all of the tRNA cross-linking to 16S rRNA is in the nucleotide interval 1394−1417 in 16S rRNA (T. Shapkina and S. Kirillov, unpublished data).

The cross-linked RNA samples containing the 3′[^{32}P]-labeled tRNA were analyzed by partial hydrolysis to determine the location of the cross-link in the tRNA (Figure 5C). Control 3′[^{32}P]-labeled unirradiated tRNA was subjected to partial RNase T1 digestion and partial hydrolysis to help determine the sites of cross-linking. In the samples from RNA 1 and 2, the pattern of tRNA partial hydrolysis matched the pattern seen in the control tRNA, but it terminated at nucleotide G34, indicating that they both have a cross-link at U33.

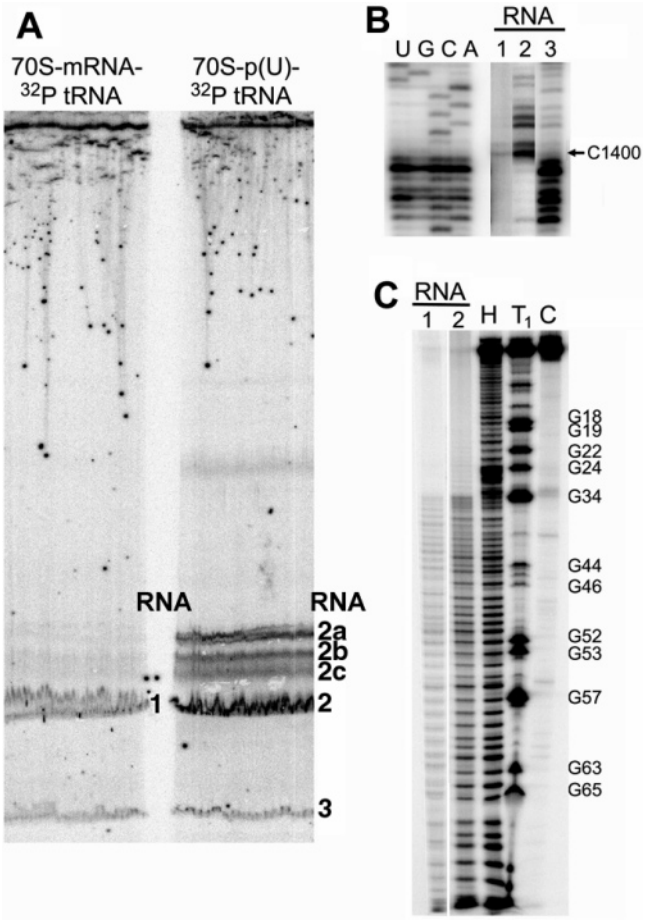

FIGURE 5: Analysis of 16S rRNA × $tRNA^{Phe}$ cross-links. (A) Denaturing polyacrylamide gel electrophoresis of RNA from irradiated complexes containing 70S, 3′[^{32}P]-labeled deacyl-$tRNA^{Phe}$ and mRNA or poly(U). RNA from bands labeled 1, 2, and 3 were isolated from the gel for further study. (B) Reverse transcription analysis on RNA samples 1−3 in the interval 1391−1409. The reverse transcription stop at G1401 at the position of the arrow indicates the cross-link at C1400 present in RNA from bands 1 and 2 but not 3. The reduced signal in lane 1 occurs because of the small amount of RNA recovered from that region of the gel, and the large signal in lane 3 is due to the large amount of linear unlabeled 16S rRNA from region 3 of the gel. (C) Partial hydrolysis analysis of the cross-linking sites in tRNA. Samples 1 and 2 were subjected to partial hydrolysis and were electrophoresed with control [^{32}P]-labeled tRNA samples to determine the sites of cross-linking. H and T1 lanes contain [^{32}P]-labeled tRNA subjected to partial hydrolysis or partial digestion with RNase T1, respectively. The lane C contains the [^{32}P]-labeled tRNA with no additional treatment. The sequence is numbered as indicated by the G residues.

DISCUSSION

These experiments were conducted to determine if there were changes in the UV-induced cross-links in the 16S rRNA within the 70S ribosome upon elongator tRNA binding that might indicate a conformational adjustment in the 30S subunit. $tRNA^{Phe}$ binding affected the intramolecular cross-link between C967 and C1400 but not others in the decoding region or elsewhere. For *N*-acetyl-Phe-$tRNA^{Phe}$, which binds to the P/P-site (*2*), the decrease in the C967 × C1400 cross-link frequency was directly proportional to the amount of tRNA bound with either poly(U) or the mRNA analogue. In the case of deacyl-$tRNA^{Phe}$, which should bind to the P/E-site or P/P-site depending on the buffer conditions (*32*), the

relationship was proportional in the presence of poly(U) but, under mRNA dependent conditions, was less than expected when the mRNA analogue was used. We previously determined that the response for initiator $tRNA^{fMet}$ binding to the 30S subunit resulted in a decrease in the C967 × C1400 cross-link (*44*), but the extent of decrease was less than even the decrease induced by deacyl-$tRNA^{Phe}$ in the presence of the mRNA analogue that was observed in these experiments. These data indicate that the geometry around C967 and C1400 is altered by tRNA, but the extent of the change depends on the identity of the tRNA and on the type of mRNA in the complex.

The degree of the C967 × C1400 cross-link inhibition for $tRNA^{Phe}$ binding in 70S ribosomes did not depend on the use of the conventional versus polyamine buffers. Cryo-EM observations made by Agrawal et al. (*32*) indicated that conventional and polyamine buffers affect the equilibrium between the P/P versus P/E arrangement, and as a consequence, in polyamine buffer the tRNA position on the 50S subunit is shifted about 30 Å toward protein L1 as compared to its arrangement in conventional buffer. However, the tRNA shift does not alter the position of the anticodon loop in the 30S subunit (*32*), and this is consistent with the similar C967 × C1400 cross-link frequency response in those buffer systems. Additional experiments done in conventional buffers with high Mg^{2+} concentration that allow mRNA-independent tRNA binding show that the inhibition of the C967 × C1400 cross-link is correlated to the $tRNA^{Phe}$ binding stoichiometry regardless of the presence of mRNA. This indicates that the alteration of the geometry is attributable to the tRNA. In addition, high Mg^{2+} changes the C967 × C1400 cross-link frequency response to make it proportional to the tRNA stoichiometry.

The C967 × C1400 cross-link observed in *E. coli* is present in other eubacteria. A cross-link identical to *E. coli* C967 × C1400 is seen in *Bacillus subtilis* 16S rRNA (*45*) and irradiation of ribosomes from *Thermus aquaticus* (*45*) and *Thermus thermophilus* (unpublished results) result in cross-linked 16S rRNA with species that have electrophoretic mobilities and reverse transcription stops at C1400 similar to those seen in *E. coli*. In both *Thermus* species, however, G966 is hypermodified, preventing reverse transcription analysis of the C967-site. In addition, complexes with *T. thermophilus* 70S ribosomes and poly(U) and tRNA and have been analyzed, and the long-range cross-link containing C1400 was specifically inhibited (unpublished results).

There is ample biochemical and structural evidence for the involvement of the 966/967 and 1400/1401 intervals in interactions with the anticodon loop of the tRNA in the P-site. G966 and C1401 both are protected from chemical modification by tRNA bound in the P-site (*2*, *24*), and modification at either of those positions interferes with mRNA-dependent tRNA P-site binding (*46*). Also, diazirine-derivatized nucleotide 32 in $tRNA^{Arg}$ has been shown to cross-link to 16S rRNA nucleotide G966 (*47*). Cross-linking of 16S rRNA nucleotide C1400 to position 34 in acetylvalyl-$tRNA_1^{Val}$ (*48*) is very efficient (*49*). In the present experiments, we have demonstrated a cross-link between 16S rRNA (at C1400) and tRNA (at U33). This is identical to the cross-link detected between 16S rRNA and $tRNA^{fMet}$, which also involves the nucleotide adjacent to the first nucleotide of the anticodon (*44*). These are different than the high-frequency cross-link made between C1400 and the modified U34 of acetylvalyl-$tRNA_1^{Val}$ (*48*), but it still is consistent with the proximity of C1400 and U33/U34 in the tRNA anticodon loop.

Crystal structures of *T. thermophilus* 70S and 30S ribosomes show the details of the interactions of 966 and 1400 with the tRNA anticodon. The 70S crystal structure was determined with complexes that contained $tRNA^{Phe}$ (*4*, *6*), and in the 30S crystal structure, each 30S subunit has a hairpin from an adjacent 30S subunit bound in the P-site (*7*, *50*). Therefore, both of the structures represent the 30S subunit with an occupied P-site. Cate et al. (*4*) described six RNA bridges between 16S rRNA and tRNA anticodon stem/loop, two of them to the anticodon. Yusupov et al. (*6*) identified those two contacts as the 16S rRNA G966 base interacting with tRNA nucleotide 34 backbone and the C1400 base stacking onto the tRNA nucleotide 34 base. From the 30S crystal structure, Carter et al. (*5*) described a possible van der Waals interaction between the G966 base and the mRNA-anticodon base-pair and a stacking interaction between C1400 and the base that corresponds to the tRNA nucleotide 34 base.

The arrangement of C967, C1400, and the tRNA anticodon stem in the *T. thermophilus* 16S rRNA (*50*) is shown in Figure 6. In this structure, G966, C967, and A968 (yellow, red, and yellow) are stacked together and are separated from C1400 (blue) by the cleft between the top of helix 44 (green) and the loop of helix 31 (yellow-green). The measured distances from C1400 (midpoint between C5 and C6) to G966 (midpoint between N7 and C8) and C967 (midpoint between C5 and C6) and A968 (midpoint between N7 and C8) are 9.4, 12.1, and 15.1 Å, respectively. These atoms were picked for distance measurement because these cross-links are all formed with UV light in the range of 250−300 and are photoreversed with UV light in the same range, indicating the presence of cyclobutane or azocyclobutane photodimers (*51*). These types of photodimers are known to involve the C5−C6 atoms in pyrimidines and the N7−C8 atoms in purines (*52*, *53*).

The cross-link C967 × C1400 made in the empty ribosome would require a C967 to C1400 distance smaller than seen in the crystal structure and disruption of the G966/C967/A968 stack. Twelve of 18 long-range UV-induced cross-links detected in *E. coli* 16S rRNA occur at C5/C6−C5/C6 or C5/C6−N7/C8 distances of 3.7−7.9 Å (average 5.5 ± 1.4 Å) in the *T. thermophilus* atomic structure; this indicates an average distance between the bonds that participate in UV-induced cross-linking (unpublished results). If this distance were the case for C967 and C1400, their separation would be about 7 Å closer in the empty 70S ribosome than they are in the crystal structure. There is evidence from cryo-EM for structural changes in this region of the subunit. Lata et al. (*56*) and Agrawal et al. (*13*) compared the 30S conformation in 30S subunits and in 70S ribosomes by cryo-EM and described a tipping of the head and rising of the shoulder of the 30S subunit to decrease the space between the head and the shoulder enough to create a channel for the mRNA at a position close to the tRNA A-site. The closing of the distance between C967 and C1400 during subunit association may be part of that change and would be consistent with the increase in the C967 × C1400 cross-link frequency in 70S ribosomes as compared to 30S subunits. Ogle et al. (*9*) and Baucom and Noller (*57*) in

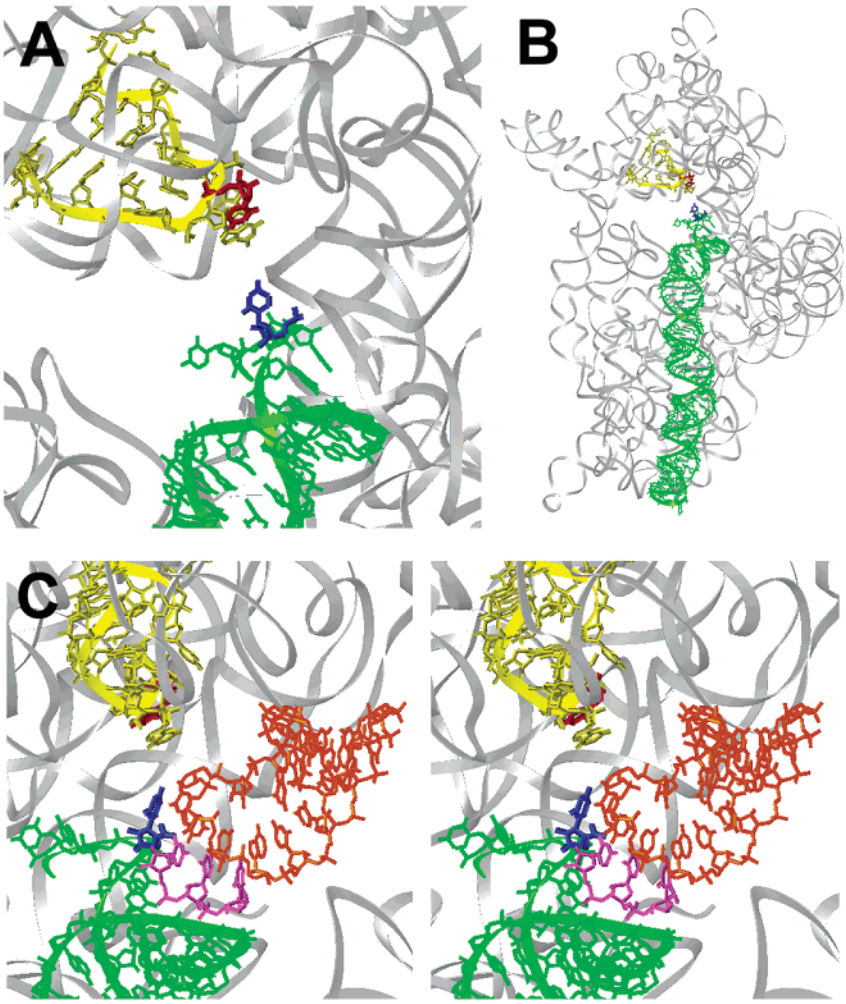

FIGURE 6: Arrangement of G966-A968, C1400, and tRNA in the 30S subunit. The 16S rRNA structure, determined by Wimberly et al. (*50*) that represents the 30S subunit with a filled P-site. The orientation is a view with the 30S interface side facing the viewer in panels A and B. The 16S rRNA backbone is shown in a gray ribbon except for helix 31 (yellow) and helix 44 (green). The positions of G966 (yellow), C967 (red), A968 (yellow), and C1400 (blue) are shown in a close view in panel A and in the long view in panel B, in which G966−A968 and C1400 are approximately in the same plane. (C) Stereoview of the P-site including the location of the tRNA analogue. The view, which looks at the tRNA P-site from the direction of the tRNA A-site, is approximately 90° to that in panel A. The tRNA analogue is orange, and the mRNA codon is purple. The program RIBBONS (*58*) was used for the illustration.

comparing the crystal structures obtained for 30S subunits in different complexes have discussed 30S movements that included tipping and rotation of the head with respect to the body and changes in the decoding region during subunit association and during tRNA A-site binding that also must involve differences in the proximity of C967 and C1400.

The conformational difference between the ribosome with the P-site filled and the empty ribosome may involve changes in addition to the domain movement of the 30S subunit head. In the presence of tRNA, nucleotides G966, C967, and A968 are stacked together with G966 extending out from the helix 31 end-loop in a position close to tRNA nucleotide 33 and C1400. This makes it more likely that G966 would be able to interact with C1400 because of its position and because C967 is sandwiched between G966 and A968 in this arrangement (Figure 6). The exclusive participation of C967 with C1400 rather than G966 with C1400 would require a disruption of the 966−968 stack in the empty ribosome to allow access to C967. A reorientation of the base of C967 would also be needed to allow for the alignment of its base and the C1400 base needed for photoaddition.

There are several possibilities for the functional significance of the alternate 30S arrangement. The C967 × C1400 cross-link does not arise merely from conformational heterogeneity in the 70S ribosome. The frequency of the cross-link is higher in the 70S ribosome than in the 30S subunit (*33*), but there is less conformational flexibility in the 70S ribosome than in the isolated 30S subunit (*13*, *54*, *55*). The C967 × C1400 cross-link also is dependent on the Mg^{2+} concentration, increasing as the Mg^{2+} concentration increases up to 20 mM (33). Therefore, the 30S arrangement associated with the cross-link is part of the default structure in the empty 70S ribosome rather than arising from a general increased flexibility. If the subunit adopts this arrangement or even undergoes part of the conformational change to decrease the C967 to C1400 distance of 12.1 Å present in the structure with P-site bound tRNA bound, or undergoes a structural change to alter the 967−969 base stacking arrangement, it would likely affect critical contacts between the 16S rRNA and the tRNA.

ACKNOWLEDGMENT

We thank Linda Spremulli and James Bullard for their generous gift of a bovine mitochondrial tRNA synthetase clone and Cindy Hemenway for a valuable critique of the manuscript.

REFERENCES

1. Moazed, D., and Noller, H. F. (1986) Transfer RNA shields specific nucleotides in 16S ribosomal RNA from attack by chemical probes, *Cell 47*, 985−994.
2. Moazed, D., and Noller, H. F. (1990) Binding of tRNA to the ribosomal A and P-sites protects two distinct sets of nucleotides in 16S rRNA, *J. Mol. Biol. 211*, 135−145.
3. Noller, H. F., Green, R., Heilek, G., Hoffarth, V., Huttenhofer, A., Joseph, S., Lee, I., Lieberman, K., Mankin, A., Merryman, C., Powers, T., Puglisi, E., Samaha, R., and Weiser, B. (1995) Structure and function of ribosomal RNA, *Biochem. Cell. Biol. 73*, 997−1009.
4. Cate, J. H., Yusupov, M. M., Yusupova, G. Z., Earnest, T. N., and Noller, H. F. (1999) X-ray crystal structures of 70S ribosome functional complexes, *Science 285*, 2095−2104.
5. Carter, A. P., Clemons, W. M., Brodersen, D. E., Morgan-Warren, R. J., Wimberly, B. T., and Ramakrishnan, V. (2000) Functional insights from the structure of the 30S ribosomal subunit and its interactions with antiobiotics, *Nature 407*, 340−348.
6. Yusupov, M. M., Yusupova, G. Zh., Baucom, A., Lieberman, K., Earnest, T. N., Cate, J. H. D., and Noller, H. F. (2001) Crystal Structure of the Ribosome at 5.5 Å Resolution, *Science 292*, 883−896.
7. Schluenzen, F., Tocilj, A., Zarivach, R., Harms, J., Gluehmann, M., Janell, D., Bashan, A., Bartels, H., Agmon, I., Franseschi, F., and Yonath, A. (2000) Structure of functionally activated small ribosomal subunit at 3.3 Å resolution, *Cell 102*, 615−623.
8. Ogle, J., Brodersen, D., Clemons, W., Jr., Tarry, M., Carter, A., and Ramakrishnan, V. (2001) Recognition of cognate transfer RNA by the 30S ribosomal subunit, *Science 292*, 897−902.
9. Ogle, J. M., Murphy, F. V., Tarry, M. J., and Ramakrishnan, V. (2002) Selection of tRNA by the ribosome requires a transition from an open to a closed form, *Cell 111*, 721−732.
10. Valle, M., Sengupta, J., Swami, N. K., Grassucci, R. A., Burkhardt, N., Nierhaus, K. H., Agrawal, R. K., and Frank, J. (2002) Cryo-EM reveals an active role for aminoacyl-tRNA in the accommodation process, *EMBO J. 13*, 3557−3567.
11. Yarus, M., Valle, M., and Frank, J. (2003) A twisted tRNA intermediate sets the threshold for decoding, *RNA 9*, 384−385.
12. Nissen, P., Hansen, J., Ban, N., Moore, P. B., and Steitz, T. A. (2000) The structural basis of ribosome activity in peptide bond synthesis, *Science 289*, 920−930.
13. Agrawal, R. K., Latta, R. K., and Frank, J. (1999b) Conformational variability in *Escherichia coli* 70S ribosome as revealed by 3-D cryo-electron microscopy, *Intl. J. Biochem. Cell Biol. 31*, 243−254.
14. Frank, J. (2003) Electron microscopy of functional ribosome complexes, *Biopolymers 68*, 223−233.
15. Frank, J., and Agrawal, R. (2000) A ratchet-like intersubunit reorganization of the ribosome during translocation, *Nature 406*, 318−322.
16. Stark, H., Rodnina, M. V., Wieden, H. J., van Heel, M., and Wintermeyer, W. (2000) Large-scale movement of elongation factor G and extensive conformational change of the ribosome during translocation, *Cell 100*, 301−309.
17. McCutcheon, J. P., Agrawal, R., Philips, S., Grassucci, R., Gerchman, S., Clemons, W., Jr., Ramakrishnan, V., and Frank, J. (1999) Location of translational initiation factor IF3 on the small ribosomal subunit, *Proc. Natl. Acad. Sci. U.S.A. 96*, 3401−4306.
18. Zamir, A., Miskin, R., and Elson, D. (1971) Inactivation and reactivation of ribosomal subunits: amino acyl-transfer RNA binding activity of the 30S subunit of *Escherichia coli*, *J. Mol. Biol. 60*, 347−364.
19. Zamir, A., Miskin, R., Vogel, A., and Elson, D. (1973) The inactivation and reactivation of *Escherichia coli* ribosomes, *Methods Enzymol. 30*, 406−426.
20. Kirillov, S. V., Makhno, V. I., and Semenkov, Y. P. (1980) Mechanism of codon-anticodon interaction in ribosomes. Direct functional evidence that isolated 30S subunits contain two codon-specific binding sites for transfer RNA, *Nucleic Acids Res. 8*, 183−196.
21. Semenkov, Y. P., Makarov, E. M., and Kirillov, S. V. (1985) Quantitative study of interaction of deacylated tRNA with the P-, A-, and E-sites of *Escherichia coli* ribosomes, *Biopolim. Kletka 1*, 183−193.
22. Zhuchenko, O. P., Semenkov, Y. P., and Kirillov, S. V. (1987) Influence of the concentration ratio of di- and univalent cations on the functional activity of *Escherichia coli* ribosome 30S subparticles, *Mol. Biol. 21*, 223−230.
23. Moazed, D., and Noller, H. F. (1989a) Interaction of tRNA with 23S rRNA in the Ribosomal A, P, and E Sites, *Cell 57*, 585−597.
24. Moazed, D., and Noller, H. F. (1989b) Intermediate states in the movement of transfer RNA in the ribosome, *Nature 342*, 142−148.
25. Pape T., Wintermeyer W., and Rodnina, M. V. (2000) Conformational switch in the decoding region of 16S rRNA during aminoacyl-tRNA selection on the ribosome, *Nat. Struct. Biol. 7*, 104−107.
26. Rodnina, M. V., Savelsbergh, A., Katunin, V. I., and Wintermeyer, W. (1997) Hydrolysis of GTP by elongation factor G drives tRNA movement on the ribosome, *Nature 385*, 37−41.
27. Jelenc, P. C., and Kurland, C. G. (1979) Nucleoside triphosphate regeneration decreases the freqency of translation errors, *Proc. Natl. Acad. Sci. U.S.A. 76*, 3174−3178.
28. Bartetzko, A., and Nierhaus, K. H. (1988) Mg^{2+}/NH_4^+/Polyamine system for polyuridine-dependent polyphenylalanine synthesis with near in vivo characteristics, *Methods Enzymol. 164*, 650−658.
29. Dabrowski, M., Spahn, C. M. T., and Nierhaus, K. H. (1995) Interaction of tRNAs with the ribosome at the A- and P-sites, *EMBO J. 14*, 4872−4882.
30. Dabrowski, M., Spahn, C. M. T., Schafer, M. A., Patzke, S., and Nierhaus, K. H. (1998) Protection patterns of tRNAs do not change during ribosomal translocation, *J. Biol. Chem. 273*, 32793−32800.
31. Spahn, C. M., and Nierhaus, K. (1998) Models of the elongation cycle: An evaluation, *Biol. Chem. 379*, 753−772.
32. Agrawal, R., Penczek, P., Grassucci, R., Burkhardt, N., Nierhaus, K., and Frank, J. (1999a) Effect of buffer conditions on the position of tRNA on the 70S ribosome as visualized by cryo-electron microscopy, *J. Biol. Chem. 13*, 8723−8729.
33. Noah, J. W., and Wollenzien, P. (1998) Dependence of the 16S rRNA decoding region structure on Mg^{2+}, subunit association, and temperature, *Biochemistry 37*, 15442−15448.
34. Noah, J. W., Dolan, M. A., Babin, P., and Wollenzien, P. (1999) Effects of tetracycline and spectinomycin on the tertiary structure of ribosomal RNA in the *Escherichia coli* 30S ribosomal subunit, *J. Biol. Chem. 274*, 16576−16581.
35. Makhno, V. I., Peshin, N. N., Semenkov, Y. P., and Kirillov, S. V. (1988) Modified method of producing "tight" 70S ribosomes from *Escherichia coli*, highly active in individual stages of the elongation cycle, *Mol. Biol. 22*, 528−537.
36. Wilms, C., Noah, J. W., Zhong, D., and Wollenzien, P. (1997) Exact determination of UV-induced cross-links in 16S ribosomal RNA in 30S ribosomal subunits, *RNA 3*, 602−612.
37. Wilms, C., and Wollenzien, P. (1994) Purification of RNA from polyacrylamide gels by ultracentrifugation, *Anal. Biochem. 221*, 204−205.
38. Rheinberger, H. J., Geigenmuller, U., Wedde, M., and Nierhaus, K. H. (1988) Parameters for the Preparation of *Escherichia coli* Ribosomes and Ribosomal Subunits Active in tRNA Binding, *Methods Enzymol. 174*, 658−670.
39. Bullard, J. M., Cai, Y. C., Demeler, B., and Spremulli, L. L. (1999) Expression and characterization of a human mitochondrial phenylalanyl-tRNA synthetase, *J. Mol. Biol. 288*, 567−577.
40. Rappoport, S., and Lapidot, Y. (1974) The chemical preparation of acetylaminoacyl-tRNA, *Methods Enzymol. 29*, 685−688.
41. Juzumiene, D., Shapkina, T., Kirillov, S., and Wollenzien, P. (2001) Short-range RNA−RNA cross-linking methods to determine rRNA structure and interactions, *Methods 25*, 333−343.
42. Moazed, D., Stern, S., and Noller, H. F. (1986) Rapid chemical probing of conformation in 16S ribosomal RNA and 30S ribosomal subunits using primer extension, *J. Mol. Biol. 187*, 399−416.
43. Juzumiene, D. I., Shapkina, T. G., and Wollenzien, P. (1995) Distribution of cross-links between mRNA analogues and 16S rRNA in *Escherichia coli* 70S ribosomes made under equilibrium conditions and their response to tRNA binding, *J. Biol. Chem. 270*, 12794−12800.

44. Shapkina, T. G., Dolan, M. A., Babin, P., and Wollenzien, P. (2000) Initiation factor3-induced structural changes in the 30S ribosomal subunit and in complexes containing $tRNA^{fMet}$ and mRNA, *J. Mol. Biol. 299*, 617−630.
45. Noah, J. W., Shapkina, T., and Wollenzien, P. (2000) UV-induced cross-links in the 16S rRNAs of *Escherichia coli*, *Bacillus subtilis*, and *Thermus aquaticus* and their implications for ribosome structure and photochemistry, *Nucleic Acids Res. 28*, 3785−3792.
46. von Ahsen, U., and Noller, H. F. (1995) Identification of Bases in 16S rRNA Essential for tRNA Binding at the 30S Ribosomal P-site, *Science 267*, 234−237.
47. Doring, T., Mitchell, P., Osswald, M., Bochkariov, D., and Brimacombe, R. (1994) The decoding region of 16S RNA; a cross-linking study of the ribosomal A-, P-, and E-sites using tRNA derivatized at position 32 in the anticodon loop, *EMBO J. 13*, 2677−2685.
48. Prince, J. B., Taylor, B. H., Thurlow, D. L., Ofengand, J., and Zimmermann, R. A. (1982) Covalent cross-linking of $tRNA_1^{Val}$ to 16S RNA at the ribosomal P-site: identification of cross-linked residues, *Proc. Natl. Acad. Sci. U.S.A. 79*, 5450−5454.
49. Schwartz, I., and Ofengand, J. (1978) Photochemical cross-linking of unmodified acetylvalyl-tRNA to 16S RNA at the ribosomal P-site, *Biochemistry 17*, 2524−2530.
50. Wimberly, B. T., Brodersen, D. E., Clemons, W. M., Morgan-Warren, R. J., Carter, A. P., Vonrhein, C., Hartsch, T., and Ramakrishnan, V. (2000) Structure of the 30S ribosomal subunit, *Nature 407*, 327−339.
51. Zhirnov, O. V., and Wollenzien, P. (2003) Action spectra for UV-light induced RNA−RNA cross-linking in 16S ribosomal RNA in the ribosome, *Photochem. Photobiol. Sci. 2*, 688−693.
52. Paszyc, S., Skalski, B., and Wenska, G. (1976) Photochemical reactions of some pyrimidine-purine dinucleotide analogues, *Tetrahedron Lett. 6*, 449−450.
53. Kumar, S., Sharma, N. D., Davies, R. J. H., Phillipson, D., and McCloskey, J. A. (1987) The isolation and characterization of a new type of dimeric adenine photoproduct in UV-irradiated deoxyadenylates, *Nucleic Acids Res*. *15*, 1199−1216.
54. Gabashivili, I. S., Agrawal, R. K., Grassucci, R., and Frank, J. (1999) Structure and structural variations of the *Escherichia coli* 30S ribosomal subunit as revealed by three-dimensional cryo-electron microscopy, *J. Mol. Biol*. *286*, 1285−1291.
55. Juzumiene, D. I., and Wollenzien, P. (2001) Arrangement of the central pseudoknot region of 16S rRNA in the 30S ribosomal subunit determined by site-directed 4-thiouridine cross-linking, *RNA 7*, 71−84.
56. Lata, K. R., Agrawal, R. K., Penczek, P., Grassucci, R., Zhu, J., and Frank, J. (1996) Three-dimensional reconstruction of the *Escherichia coli* 30S ribosomal subunit in ice, *J. Mol. Biol. 262*, 43−52.
57. Noller, H. F., and Baucom, A. (2002) Structure of the 70S ribosome: implications for movement, *Biochem. Soc. Trans. 30*, 1159−1161.
58. Carson, M. (1991) Ribbons 2.0, *J. Appl. Crystallogr. 24*, 958−961.

BI035369Q